buildings

MDPI

Article

Study on the Impact of Temperature and Humidity Variations in Climate Zones on the Life-Cycle Assessment of Wall Materials

Xiling Zhou [1], Xinqi Wang [1], Linhui Wan [1], Yuyang Chen [1], Xiaohua Fu [2] and Yi Wu [1,*]

[1] College of Water Resources and Civil Engineering, Hunan Agricultural University, Changsha 410128, China; zhouxiling@hunau.edu.cn (X.Z.); XinQiWang@stu.hunau.edu.cn (X.W.); wanlinhui08@hunau.edu.cn (L.W.); 3215673306@stu.hunau.edu.cn (Y.C.)

[2] School of Ecology and Environment, Central South University of Forestry & Technology, Changsha 410004, China; T20031513@csuft.edu.cn

* Correspondence: xhwuyi@hunau.edu.cn; Tel.: +86-13755062068

Abstract

Life-cycle assessment is crucial for evaluating materials' environmental impact and guiding the development of low-carbon and sustainable buildings. However, conventional LCA methods often overlook critical impacts during the operation and maintenance stage. To address this gap, this study proposes an improved framework using four composite indicators to enable systematic evaluation of six wall materials across China's five climate zones. Using a university teaching building in the Hot Summer and Cold Winter Zone as a case study, this study quantitatively analyzed the economic viability and carbon reduction potential of each material. Results indicate that lower thermal conductivity does not necessarily imply superior economic and carbon reduction performance. Factors including the material carbon emission factor, cost, and thermal properties, must be comprehensively considered. Buffering materials also exhibit climate dependency—WPM and BWPM (moisture-buffering plastering mortars) perform better in hot–humid zones than temperate zones. All five buffer materials reduce operational energy consumption; WPM and BWPM stand out with 15.7% and 16.7% life-cycle cost savings and 17.3% and 18.0% carbon emission reductions, respectively. This study addresses the limitations of traditional LCC/LCA and provides theoretical and practical support for scientific material selection and low-carbon building design.

Keywords: life-cycle assessment indicators; wall materials; comprehensive assessment indicators

1. Introduction

The World Meteorological Organization (WMO) confirmed 2024 as the warmest year on record, with the global mean near-surface temperature 1.55 °C above the 1850–1900 pre-industrial baseline [1]. This intensifying climate crisis has placed greenhouse gas (GHG) mitigation at the forefront of global concerns [2]. The construction sector accounts for approximately 40% of global final energy use and 33% of energy-related carbon dioxide emissions [3]. In China, the building life-cycle carbon footprint accounts for approximately 51% of the national total, with the materialization, construction, and operation stages contributing 28.3%, 1.7%, and 21.6%, respectively [4]. Against this backdrop, advancing building energy conservation and low-carbon transition is imperative for mitigating climate change.

The building envelope, as the primary physical barrier between indoor and outdoor environments, is a key determinant of building energy efficiency [5]. In recent years, wall

Check for updates

Received: 10 December 2025
Revised: 8 January 2026
Accepted: 13 January 2026
Published: 16 January 2026

Copyright: © 2026 by the authors. Licensee MDPI, Basel, Switzerland. This article is an open access article distributed under the terms and conditions of the Creative Commons Attribution (CC BY) license.

buffering materials have attracted considerable attention due to their potential to improve energy efficiency, enhance indoor comfort, and reduce carbon emissions [5,6]. Research indicates that indoor humidity not only directly affects heating and cooling loads [7,8] but is also closely associated with mold growth on indoor surfaces [9,10]. Moreover, inappropriate humidity levels can adversely affect occupants' respiratory health and immune function [11–13]. These factors collectively underscore the growing importance of developing buffering wall materials with autonomous humidity regulation capabilities to support healthier and sustainable buildings.

By composition, thermal insulation materials can generally be classified into board-type and cement-based buffering materials. Common board-type buffering materials include extruded polystyrene (XPS) boards [14,15], expanded polystyrene (EPS) boards [16,17], polyurethane (PU) foam [18], rock wool boards [19], and phenolic resin foam [20–22]. Most of these are organic materials. Among them, XPS and EPS boards have gained widespread application due to their favorable combination of light weight, high insulation efficiency, cost-effectiveness, and ease of installation.

Cement-based buffering materials include expanded perlite mortar [23], foamed concrete [24], vitrified microsphere mortar [25,26], and ceramsite concrete [27]. Among these, expanded perlite mortar (EM) is the most widely used cement-based thermal insulation material due to its excellent fire and mold resistance, ease of installation, and cost-effectiveness [28,29].

With technological advancements, a new type of cement-based buffering material—moisture buffering plastering mortar—has emerged in recent years. As an emerging smart building material, it can stabilize indoor humidity through a dynamic bidirectional regulation mechanism. Its operation relies on autonomous moisture response: when the ambient relative humidity rises above a critical threshold, water vapor is spontaneously adsorbed into the material's microporous structure; conversely, the stored moisture is released when the humidity drops. This reversible process enables adaptive indoor environmental regulation without external energy input [30–32]. Due to its unique ecological regulation capability, this type of mortar has become a core component in passive energy-saving building design.

The extended lifespan and multiple stages of buildings make it crucial to conduct a life-cycle carbon emissions analysis of building materials. This analysis helps accurately quantify emissions across all stages and supports the formulation of carbon management strategies [33]. Life-Cycle Assessment (LCA) is an internationally recognized, comprehensive method for evaluating the environmental impacts of products and technologies. It is widely applied in the engineering and materials fields [34]. It divides the life-cycle into three stages: materialization, operation and maintenance, and dismantling and disposal. The system boundary encompasses the entire process from raw material acquisition to final disposal.

Common metrics include Life-Cycle Assessment (LCA) [35], Life-Cycle Cost (LCC) [36], and Life-Cycle Sustainability Assessment (LCSA). The LCA method quantifies the environmental impacts of products, processes, or systems by statistically analyzing inputs, outputs, and potential effects throughout their life-cycle. This method covers the entire life-cycle, from raw material extraction ("cradle") to use and final disposal ("grave"), offering a comprehensive perspective on environmental impacts. It serves as a core tool for sustainability assessments [34–36]. Life-Cycle Cost (LCC) evaluates the total economic expenditure of a product, project, or system throughout its entire life-cycle, encompassing initial investment, installation, and subsequent operational, maintenance, replacement, and disposal costs [34,37]. Life-Cycle Sustainability Assessment (LCSA) provides a holistic framework for evaluating the comprehensive sustainability impacts of a product or project.

It integrates three core dimensions: environmental (through LCA), economic (through LCC), and social (through social LCA) [38,39].

Building upon this foundation, two key evaluation metrics have been further derived: Carbon Emission Payback Period and Avoided Carbon Emission. The former refers to the time required for the carbon emissions reduced through energy savings during the operational stage of a material to fully offset the embodied carbon generated during its production and construction processes [40]. The latter refers to the total reduction in carbon emissions achievable over the entire life-cycle through the adoption of high-performance materials or technologies [41,42]. These two approaches provide a basis for assessing the long-term carbon benefits of building materials by quantitatively evaluating dynamic efficiency over time and overall scale.

However, while traditional LCA methods encompass the entire life-cycle, when applied to construction, they often treat building materials as static "commodities". These methods primarily account for the direct costs and environmental impacts incurred during the production, transportation, construction, and dismantling processes of the materials. The operation and maintenance stage is considered a distinct stage, primarily determined by energy consumption resulting from equipment use.

To address this shortcoming, this study refines and extends the conventional LCC and LCA methods by proposing four integrated evaluation indicators: Energy-Saving Economic Equivalent (C_{loss}), Energy-Saving Carbon Emission Reduction Equivalent (CE_{loss}), Economic Payback Period ($C_{payback}$), and Carbon Emission Payback Period ($CE_{payback}$). The core methodological innovation lies in explicitly quantifying how material properties enhance building operational energy efficiency and then translating this improvement into a net beneficial performance metric. This metric, expressed in both economic and carbon terms, represents the material's net positive contribution that can be directly offset against the burdens (costs and embodied carbon) incurred during its production, construction, and demolition stages.

This approach enables a precise assessment of a building material's net life-cycle contribution, going beyond traditional stage-isolated evaluations. Based on this indicator system, six typical wall materials—including board-type buffering materials, cement-based buffering materials, and a control group with common plastering mortar (CM)—were selected for horizontal comparative evaluation across China's five climatic zones. The aim was to reveal the interaction between climatic differences and material properties. Meanwhile, using a university teaching building in the Hot Summer and Cold Winter Zone as a practical case, this study quantitatively evaluated the performance of various materials in real buildings through refined simulation and calculation to verify the practicality and effectiveness of the proposed indicator system. This study aims to provide a novel quantitative analysis tool for the scientific selection of wall materials and key methodological support for improving green building material evaluation standards.

2. Methods and Materials

2.1. Methods

To comprehensively evaluate the impact of materials across the building life-cycle, this study proposes a framework comprising four integrated evaluation indicators to assess the economic viability and carbon-reduction potential of materials, as shown in Table 1.

Table 1. The significance of the four evaluation indicators and their inter-relationships.

	Name	Symbol	Meaning
Economic Dimension	Energy-Saving Economic Equivalent	C_{loss}	Used to evaluate the impact of materials on the total life-cycle cost of a building.
	Economic Payback Period	$C_{payback}$	The time required for the cumulative energy savings achieved during the operational stage to offset the material costs.
Carbon Reduction Dimension	Energy-Saving Carbon Emission Reduction Equivalent	CE_{loss}	Used to assess the impact of materials on carbon emissions throughout the building's entire life-cycle.
	Carbon Emission Payback Period	$CE_{payback}$	The time required for carbon emissions saved during the operational stage to offset material-related carbon emissions.

The Energy-Saving Economic Equivalent (C_{loss}) is calculated as shown in Equation (1). Apart from covering the costs incurred during the materialization stage and the demolition and disposal stage, it also takes into account the energy consumption changes resulting from the use of materials during the building's operation and maintenance stage, converting these into associated economic costs.

$$C_{loss} = C_{h=0} - C_{Material} \quad (1)$$

where C_{loss} is the Energy-Saving Economic Equivalent, CNY; $C_{Material}$ refers to the life-cycle cost of a material, covering the materialization, operation and maintenance, and demolition and disposal stages, CNY. Among these, the operation and maintenance stage includes expenses for the materials' replacement and energy consumption costs for building operation when using these materials. $C_{h=0}$ represents the building operational energy consumption when this material is not used (i.e., the material thickness is 0), CNY.

When C_{loss} is greater than 0, it indicates that the reduction in electricity costs from the material's improved thermal performance exceeds the materials' life-cycle investment, demonstrating the material's economic viability. If C_{loss} is less than 0, it indicates that total investment exceeds operational energy savings generated, rendering the material economically unfeasible.

The Economic Payback Period ($C_{payback}$) is calculated as shown in Equation (2). Specifically, it denotes the duration needed for energy cost savings from improved building envelope performance to offset the cost of employed materials.

$$C_{payback} = \frac{\Delta C_{O\&M}}{C_{Mat} + C_{D\&D}} \quad (2)$$

where $C_{payback}$ denotes the Economic Payback Period, Year; $\Delta C_{O\&M}$ represents the annual difference in operation and maintenance costs between using this material and not using it during the operational stage, with the unit of CNY·Year; C_{Mat} refers to the material cost during the materialization stage, CNY; $C_{D\&D}$ denotes the material cost during the demolition and disposal stage, CNY.

When $C_{payback}$ does not exceed the structure's design service life, the material is deemed to have economically viable. Under such conditions, the shorter the $C_{payback}$, the faster the investment recovery and the greater the economic benefits.

The Energy-Saving Carbon Emission Reduction Equivalent (CE_{loss}) is calculated as shown in Equation (3). In addition to encompassing carbon emissions incurred during material production and construction stages, it also includes energy consumption changes

from material's usage during building operation and maintenance stage, converting these into associated carbon emissions.

$$CE_{loss} = CE_{h=0} - CE_{Material} \quad (3)$$

where CE_{loss} denotes the Energy-Saving Carbon Emission Reduction Equivalent, tCO_2e; $CE_{Material}$ refers to the material's life-cycle carbon emission, covering the materialization, operation and maintenance, and demolition and disposal stages, tCO_2e. Among these, the carbon emissions during the operation and maintenance stage include those generated by material maintenance and the carbon emissions associated with energy consumption when the material is used in the building; $CE_{h=0}$ represents the carbon emissions during the operation and maintenance stage when the material is not used, tCO_2e.

A positive CE_{loss} indicates carbon reduction feasibility, meaning life-cycle CO_2e savings surpass the material's own embodied emissions. The magnitude of CE_{loss} directly reflects the material's carbon reduction potential. A negative CE_{loss}, however, signifies the material generates more emissions than it saves, indicating it lacks carbon reduction potential.

The Carbon Emission Payback Period ($CE_{payback}$) is calculated as shown in Equation (4). Specifically, it denotes the duration required for energy-related carbon emission reductions resulting from improved building envelope performance to offset the material's embodied carbon emissions.

$$CE_{payback} = \frac{\Delta CE_{O\&M}}{CE_{Mat} + CE_{D\&D}} \quad (4)$$

where $CE_{payback}$ denotes the Carbon Emission Payback Period, Year; $\Delta CE_{O\&M}$ represents the annual difference in carbon emissions during the operational stage between the scenario with this material and without it, $tCO_2e{\cdot}Year$; CE_{Mat} refers to the material-related carbon emissions during the materialization stage, tCO_2e. $CE_{D\&D}$ denotes the material-related carbon emissions during the demolition and disposal stage, tCO_2e.

When $CE_{payback}$ does not exceed the material's design service life, this material is deemed to have carbon reduction potential. Under such conditions, the shorter the $CE_{payback}$, the faster the carbon emission offset, and the greater the carbon reduction potential.

This framework broadens the perspective and system boundaries for evaluating building materials. Traditional approaches, while covering the entire life-cycle, typically treat materials as static "commodities". They focus on calculating the direct costs and carbon emissions associated with the materialization, transportation, construction, and demolition stages, while treating the operation and maintenance stage as a separate component. The core breakthrough of this framework lies in internalizing the impact of a material's thermal properties on a building's long-term operational energy consumption as a quantifiable attribute inherent to the material itself. Through indicators such as "Energy-Saving Economic Equivalent" and "Economic Payback Period", it calculates the net performance by comparing the energy-saving and carbon reduction benefits during the operation and maintenance stage with the implicit costs and carbon emissions associated with the materialization and demolition disposal stages. This expands the scope of evaluation from the "material's own footprint" to the "overall benefits of material use," establishing a direct link between material selection and the building's life-cycle cost and carbon emissions performance.

This study expands the Carbon Emission Payback Period and Avoided Carbon Emission. Compared to the Carbon Emission Payback Period, the Economic Payback Period builds on it by incorporating emissions from demolition and disposal, thereby establishing a more comprehensive life-cycle carbon accounting boundary. Compared to Avoided Carbon Emission, Energy-Saving Economic Equivalent integrates operational emission

reductions with carbon emissions from material production, physical transformation, demolition, and other stages into a unified calculation. This avoids the potential misdirection of focusing solely on energy savings during the operational stage, whereby excessively high embodied carbon in materials may actually prevent achieving net carbon reduction across the entire life-cycle.

2.2. Materials

This study classifies wall materials into a control group and a buffer material group, as shown in Figure 1. The control group comprises the most commonly used common plastering mortar (CM), with its mix ratio presented in Table 2. Buffering materials are further subdivided into two categories: board-type and cement-based. Board-type buffering materials include extruded polystyrene (XPS) boards and expanded polystyrene (EPS) boards. Cement-based buffering materials consist of the widely used expanded perlite insulation mortar (EM) and two high-performance moisture buffering plastering mortars developed in the research team's earlier work—wood-plastic buffering plastering mortar (WPM) and bamboo-wood-plastic buffering plastering mortar (BWPM). The compositions of the cement-based materials are provided in Table 2.

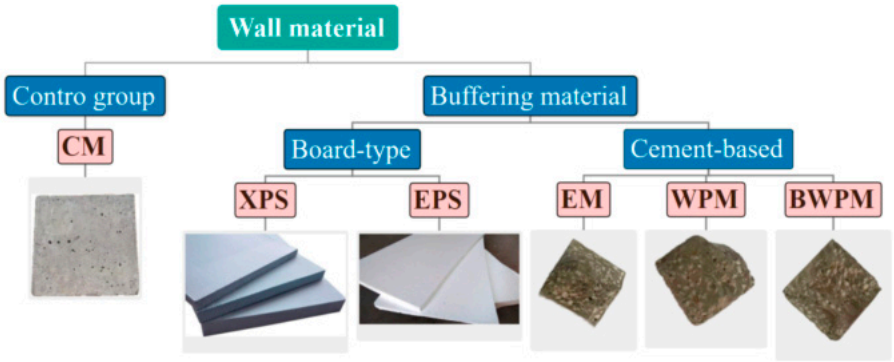


Figure 1. Material selection and classification.

Table 2. The mix ratio of cement-based materials and common mortar.

Material	Wooden Fiber (g)	Bamboo Fiber (g)	Polypropylene Fiber (g)	120-Mesh Sepiolite (g)	Diatomite (g)	Sand (g)
CM	0	0	0	0	0	300
WPM	1.462	0	3	9.435	0	
BWPM	2.580	0.206	3	5.55	40	
EM	0	0	3.2	0	0	

Material	Fly ash (g)	Expanded perlite (g)	Redispersible polymer powder (g)	Air-Entraining agent (g)	Cement (g)
CM	0	0	0	0	100
WPM	0	5.168	4	0	100
BWPM	0	9.120	4	0	100
EM	319	532	3.2	1.1	1064

The thermal insulation performance of the two groups is presented in Table 3. The WPM and BWPM data were obtained through actual measurements by the research team, while the CM, XPS, EPS, and EM data were sourced from the Thermal Design Code for Civil Buildings (GB 50176-2016 [43]). Notably, the density and thermal conductivity of the buffering materials are lower than those of the control group (CM). A lower density helps reduce the building load, while a lower thermal conductivity can substantially enhance the thermal performance of the building envelope and reduce energy consumption during the building's operation and maintenance. Additionally, the specific heat capacities of WPM and BWPM in the cement-based buffering material group are higher than those of other materials. This indicates that these two materials can store more heat and reduce indoor temperature fluctuations, creating a more comfortable thermal environment.

Table 3. Thermal insulation performance of the six materials [43].

Group	Material	Density (kg/m^3)	Thermal Conductivity (W/(m·K))	Specific Heat Capacity (J/(kg·K))
Control	CM	2000.0	1.1130	1000.0
Board-type	XPS	20.0	0.0300	1380.0
	EPS	35.0	0.0390	1380.0
Cement-based	EM	508.7	0.0974	1050.0
	WPM	784.5	0.1190	5463.8
	BWPM	754.3	0.1020	5667.0

In practical applications, WPM and BWPM can directly replace CM for wall surface finishing. For the other three buffering materials (EM, XPS, and EPS), a 20 mm thick base mortar layer is first required, followed by the application of the respective buffering materials. The application details of all six materials are illustrated in Figure 2.

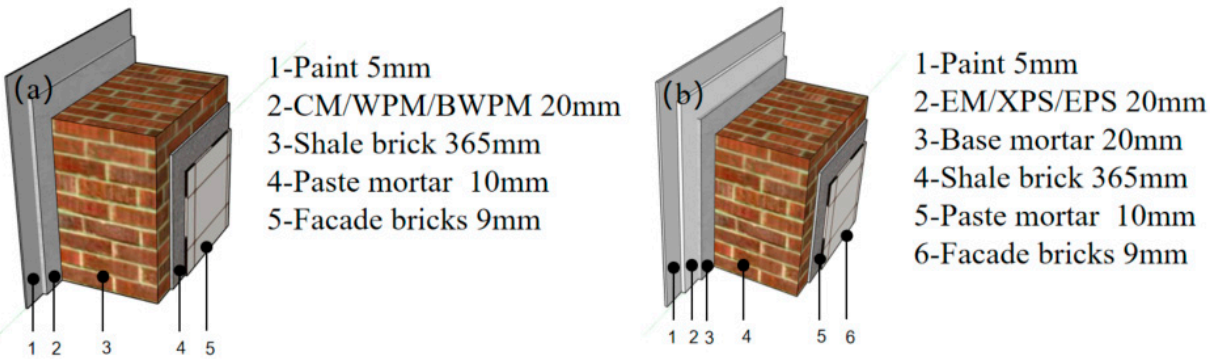


Figure 2. Schematic diagram of the construction of the six materials: (**a**) CM, WPM, BWPM, (**b**) EM, XPS, EPS.

Following extensive field investigations and market research, this study compiled cost data and carbon emission factors for the six materials, as presented in Table 4. The price of CM is calculated based on comprehensive on-site survey data from construction projects and information from the China Cement Network. Data for XPS and EPS are sourced from the "2020 Hunan Provincial Consumption Quota (Basic Price List) for Building Construction and Decoration Engineering". The carbon emission factor for CM is derived from its mix ratio, while those for EPS and XPS are from the "Standard for Building Carbon Emission Calculation" (GB/T 51366-2019 [44]).

Table 4. The carbon emission factor and production cost of the above six materials [44].

Group	Material	Carbon Emission Factor ($kgCO_2e/m^3$)	Production Price (CNY/m^3)
Control	CM	265.45	605
Board-type	XPS	296.60	283
	EPS	221.20	619
Cement-based	EM	457.20	1042
	WPM	1016.63	2317
	BWPM	612.96	1397

Regarding the carbon emission factors of WPM, BWPM, and EM, direct calculation is challenging because clear carbon emission factors are unavailable for several components in their mix ratios (e.g., bamboo fibers, polypropylene fibers, and renewable dispersible latex powder). With reference to the cost-carbon emission calculation model proposed by Fu et al. [45] and the sensitivity analysis methods [46–48], the carbon emission factors of these three materials can be approximated using Equation (5).

$$CF_i = \frac{C_i}{C_{CM}} CF_{CM} \quad (5)$$

where CF_i is the carbon emission factor of the i-th type of mortar, $kgCO_2e/m^3$; C_i is the cost of the i-th type of mortar, CNY; C_{CM} is the cost of the CM, CNY; CF_{CM} is the carbon emission factor of the CM, $kgCO_2e/m^3$.

The application of buffering materials reduces building operational energy consumption; however, it also increases carbon emissions and the costs associated with material production, transportation, construction, and demolition. Therefore, the use of buffering materials has a dual impact on the economic viability and carbon-reduction potential of buildings throughout their life-cycle.

Regarding material thickness, the "Technical specification for plasting mortar" (JGJ/T 220-2010 [49]) recommends that the average plastering thickness for walls should not exceed 20 mm. Therefore, this study sets the application thickness of all six materials to 20 mm, with the aim of conducting a consistent comparative analysis of their life-cycle impacts.

2.3. Variations in Economic and Carbon Reduction Performance Across Climate Zones

As the world's third-largest country in terms of land area, China's extensive territory gives rise to substantial climatic variations across its north–south and east–west regions [50–54]. Accord to Section 2.3, the "Design Standard for Energy Efficiency of Public Buildings" (GB 50189-2015 [55]) divides the country into five thermal design zones: Severe Cold Zone, Cold Zone, Hot Summer and Cold Winter Zone, Hot Summer and Warm Winter Zone, and Temperate Zone. The regional divisions and representative cities are illustrated in Figure 3. Given these substantial climatic disparities, the energy-saving effects of buffering materials vary across different zones in practical applications; therefore, this factor must be considered when conducting the life-cycle analyses.

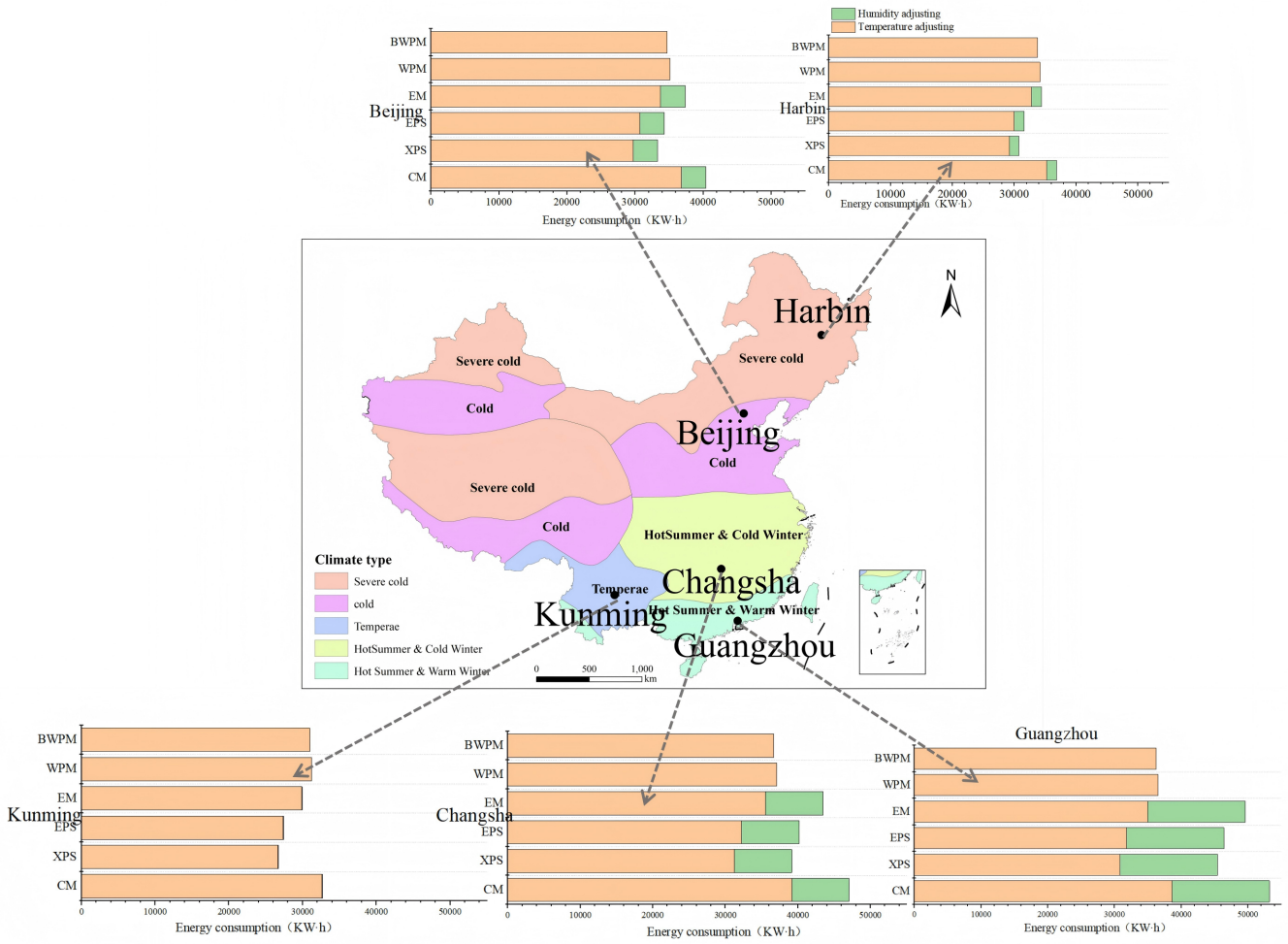


Figure 3. Energy consumption of the Figure 3 model in different climate zones and Climate Zone Classifications [55].

Air conditioning is used to control temperature. According to the Residential Building Energy Efficiency Design Standard (DB11/891-2020 [56]). The heating season runs from 15 November to 15 February, with the air conditioner set to 18 °C. The cooling season runs from 1 June to 31 August, with the air conditioner set to 26 °C. The residential building daily schedule is shown in Table 5. Currently, most energy-consumption simulations of HVAC systems during building operation and maintenance use Energy Plus [57,58]. Therefore, the air conditioning energy consumption in this study was primarily simulated using EnergyPlus 22.2.0.

Table 5. Residential building daily schedule [56].

Lighting		Equipment			Personnel	
Power Density (W/m^2)	Start Period	Power Density (W/m^2)	Start Period	Density	Heat Output (W/Person)	Air Conditioning Start Period
6	18:00–24:00	2.25	01:00–24:00	2.45 (person/household)	109	01:00–24:00

The impact of existing buffering materials on building energy consumption refers to the effect of coupled heat and moisture transfer on residential energy consumption [59]. Dehumidifiers and humidifiers are used to regulate indoor humidity; this is in accordance with the requirements for air conditioning in humid environments in areas where people stay for extended periods, as specified in the Code for "Design code for heating, ventilation,

and air conditioning of civil buildings" (GB 50736-2012 [60]). During heating, the indoor relative humidity should not fall below 30%. During cooling, the relative humidity should be maintained between 40% and 60%. Equipment selection references common market products: for dehumidification, the Midea CF20BD/N7-DA1 dehumidifier (rated power 220 W) was selected; for humidification, the Midea W40S fog-free humidifier (rated power 10 W) was selected. The Midea CF20BD/N7-DA1 dehumidifier and the Midea W40S fog-free humidifier are both manufactured by China's Midea Group, and the products are suitable for many countries and cities around the world. When relative humidity is between 60% and 80%, the dehumidification equipment operates at 60% of its rated power. When relative humidity exceeds 80%, dehumidification power increases to 90% of the rated power. The humidification equipment consistently operates at 90% of its rated power. This study assumes that temperature and humidity control equipment are activated and deactivated simultaneously. Based on hourly humidity data from each region, the energy consumption for humidity control is calculated by determining the energy usage of humidifiers and dehumidifiers. Based on hourly humidity data from various regions (sourced from rp5 [61]), the energy consumption for humidity control is calculated by the energy usage of humidifiers and dehumidifiers.

By calculation, taking the detached building shown in Figure 4 as an example, the energy consumption throughout the building's life-cycle, including the operation and maintenance stage, is shown in Figure 4. Building energy consumption originates not only from temperature control but also from humidity regulation, particularly in hot and humid climates (i.e., the Hot Summer and Cold Winter Zone and the Hot Summer and Warm Winter Zone). For instance, in Changsha and Guangzhou, the energy demand for humidity control accounts for 20% and 38% of that for temperature control, respectively. Therefore, the use of humidity-regulating materials for passive moisture management is a critical strategy for reducing the overall building energy demand. For the same building materials, energy consumption also varies across different climatic zones. Energy consumption in the Hot Summer and Warm Winter Zone and the Hot Summer and Cold Winter Zone is higher than that in the Cold Zone and the Severe Cold Zone. The Temperate Zone has the lowest energy consumption, as humidity control is rarely required there.

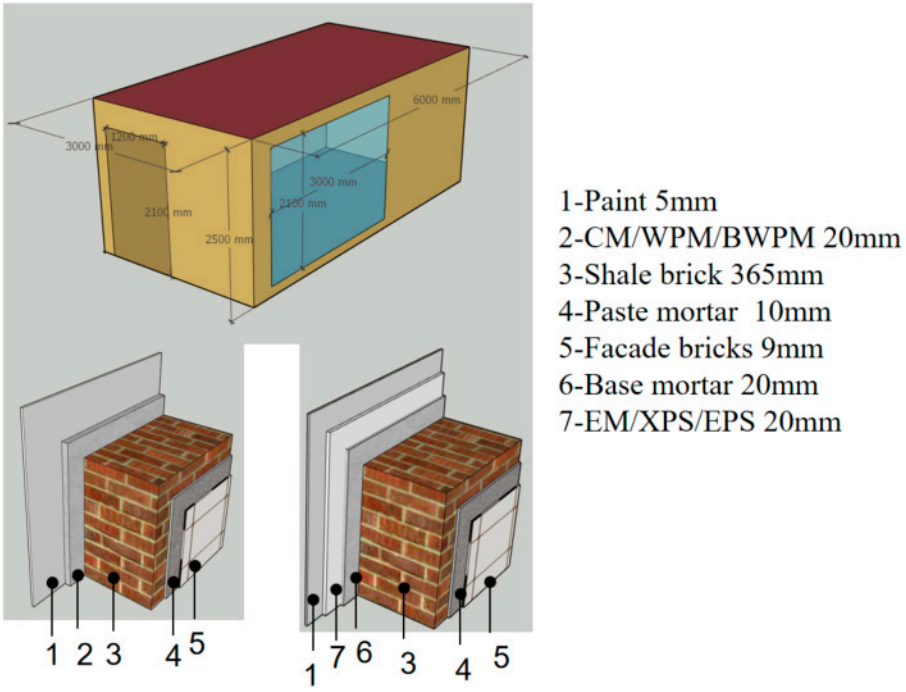


Figure 4. Residential building model.

Cement-based buffering materials, WPM and BWPM, possess dual functions: humidity regulation and thermal insulation. These materials can decrease building operational energy consumption, thus providing life-cycle economic benefits and carbon-reduction potential. In hot and humid climates (i.e., the Hot Summer and Cold Winter Zone and Hot Summer and Warm Winter Zone), WPM and BWPM exhibit a superior energy-saving performance compared to EM, board-type buffering materials, and CM. In cold, dry climates (e.g., the Cold Zone, Severe Cold Zone, and Temperate Zone), where humidity loads are moderate, energy savings mainly stem from thermal insulation performance. As a result, the energy-saving performance of board-type buffering materials is better than that of cement-based buffering materials. Overall, the energy-saving performance of buffering materials is superior to that of CM.

Different materials exhibit varying carbon emissions and costs during their materialization, operation and maintenance, demolition and disposal stages, as shown in Figures 5 and 6. However, a consistent finding is that carbon emissions and costs during the operation and maintenance stage account for nearly 90% of the life-cycle emissions and costs. This is because this stage encompasses the entire service life of the building, during which the continuous consumption of energy sources such as electricity and thermal energy leads to substantial cumulative carbon emissions and costs.

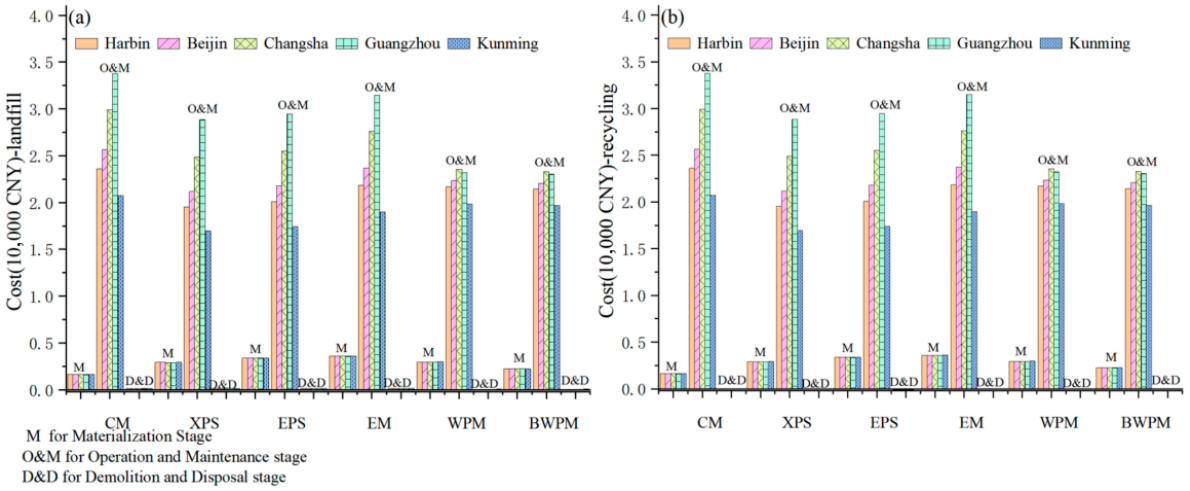


Figure 5. Life-cycle costs of different materials across various climate zones at each stage (**a**) landfill (**b**) recycling.

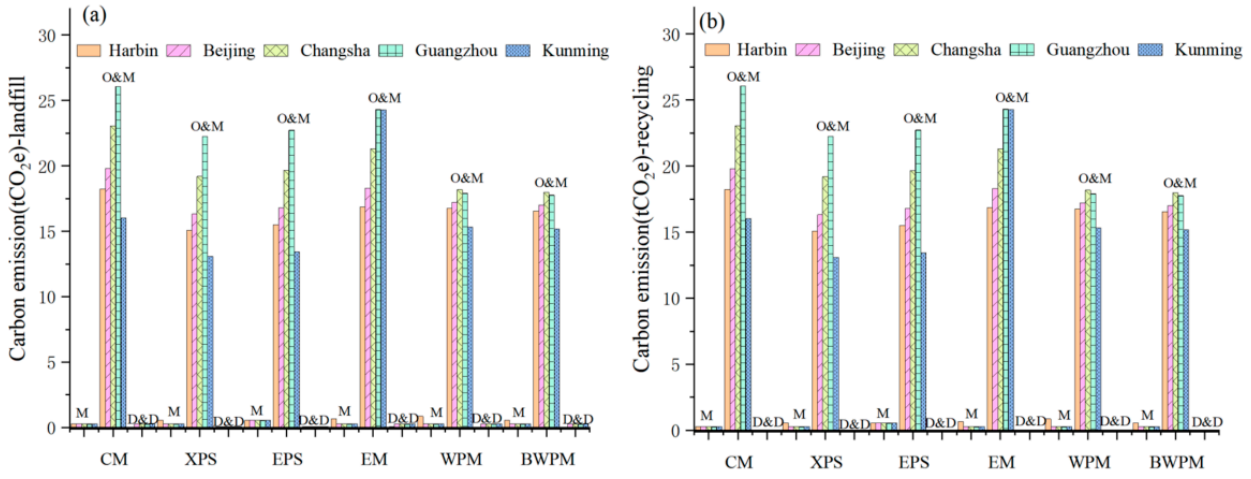


Figure 6. Life-cycle carbon emission of different materials across various climate zones at each stage (**a**) landfill (**b**) recycling.

Material recycling during the demolition and disposal stage can effectively reduce the life-cycle costs and carbon emissions of materials, thereby enhancing their economic viability and carbon reduction potential. Notably, during the operation and maintenance stage, WPM and BWPM can effectively reduce building operational energy consumption over the entire service life, further validating their application potential in the green building sector.

The four comprehensive evaluation indicators for the six materials across different climatic zones were calculated under the material recycling scenario, with the results presented in Table 6.

Table 6. Comprehensive evaluation indicators of the above six materials across different climate zones.

Region	Indicator	Control	Board-Type		Cement-Based		
		CM	XPS	EPS	EM	WPM	BWPM
Harbin	C_{loss} (10,000 CNY)	−0.18	0.10	0.01	−0.20	−0.12	−0.02
	$C_{payback}$ (Year)	−454.65	36.67	48.90	112.02	85.18	55.88
	CE_{loss} (tCO_2e)	−0.40	2.48	2.11	0.55	0.49	1.01
	$CE_{payback}$ (Year)	−97.50	8.62	9.15	27.57	31.80	17.34
Beijing	C_{loss} (10,000 CNY)	−0.18	0.15	0.04	−0.18	0.02	0.12
	$C_{payback}$ (Year)	−454.65	32.93	44.24	100.82	46.63	32.55
	CE_{loss} (tCO_2e)	−0.40	2.82	2.39	0.69	1.59	2.11
	$CE_{payback}$ (Year)	−97.50	7.74	8.28	24.81	17.41	10.10
Changsha	C_{loss} (10,000 CNY)	−0.17	0.21	0.10	−0.14	0.33	0.43
	$C_{payback}$ (Year)	−909.31	28.81	37.92	80.66	23.57	17.10
	CE_{loss} (tCO_2e)	−0.33	3.30	2.86	1.03	3.98	4.50
	$CE_{payback}$ (Year)	−195.00	6.77	7.10	19.85	8.80	5.31
Guangzhou	C_{loss} (10,000 CNY)	−0.17	0.20	0.10	−0.14	0.75	0.84
	$C_{payback}$ (Year)	−909.31	29.33	38.71	80.66	14.06	10.45
	CE_{loss} (tCO_2e)	−0.33	3.23	2.79	1.03	7.25	7.70
	$CE_{payback}$ (Year)	−195.00	6.89	7.25	19.85	5.25	3.24
Kunming	C_{loss} (10,000 CNY)	−0.19	0.07	−0.02	−0.21	−0.23	−0.14
	$C_{payback}$ (Year)	−303.10	40.33	53.09	118.61	227.98	135.49
	CE_{loss} (tCO_2e)	−0.47	2.21	1.91	0.48	−0.35	0.10
	$CE_{payback}$ (Year)	−65.00	9.48	9.94	29.19	85.11	42.04

For the control group (CM), the C_{loss} and CE_{loss} values are consistently negative across all climatic zones, while its $C_{payback}$ and $CE_{payback}$ far exceed its design service life (50 years). This means CM is neither economically viable nor effective in reducing carbon emissions over the building's service life. For the two board-type buffering materials (XPS and EPS), favorable economic and carbon-reduction performance is demonstrated across all climatic zones, with minimal variation attributed to climatic conditions.

Among the three cement-based buffering materials, the economic viability and carbon reduction potential of WPM and BWPM are sensitive to climatic conditions. In zones with lower humidity control requirements (e.g., Harbin and Kunming), their economic and carbon reduction performance is inferior to that of board-type buffering materials. This is attributed to their higher raw material costs and carbon emission factors, resulting in negative C_{loss} (indicating economic impracticability) and low CE_{loss} (reflecting low carbon reduction potential). Conversely, in hot, humid zones (e.g., Changsha and Guangzhou), the superior humidity-regulating capabilities of these two materials can reduce operational energy consumption, thereby delivering substantial carbon-reduction potential and favorable economic viability. In the Hot Summer and Warm Winter Zone, BWPM achieves C_{loss} of 43,000 CNY and CE_{loss} of 4.5 tCO_2e, vastly outperforming its performance in the Temperate Zone (C_{loss}: −14,000 CNY; CE_{loss}: 0.10 tCO_2e). In contrast, while EM exhibits excellent ther-

mal insulation performance and carbon-reduction potential, its high unit-area installation cost renders it economically unfeasible across all climatic zones. Among the six materials, WPM and BWPM demonstrate best comprehensive performance in high-humidity zones (e.g., Hunan and Guangzhou). Specifically, in the Hot Summer and Cold Winter Zone and the Hot Summer and Warm Winter Zone, their economic viability and carbon-reduction potential are superior to those of board-type buffering materials and EM, and far exceed those of the control group (CM). Conversely, in the Severe Cold Zone, Cold Zone, and Temperate Zone, the comprehensive performance of XPS, EPS, and EM outperforms that of WPM and BWPM. However, regardless of the climatic zone, the comprehensive benefits of buffering materials (both cement-based and board-type) are superior to those of CM.

Overall, the comprehensive life-cycle benefits of buffering materials cannot be determined solely by a single factor such as thermal conductivity or carbon emission factors. Instead, a systematic evaluation should be conducted by comprehensively considering multiple factors, including cost, carbon emission factors, thermal performance, and so on. The four indicators proposed in this study—C_{loss}, $C_{payback}$, CE_{loss}, and $CE_{payback}$—effectively reveal the differences in the economic and environmental performance of materials under varying climatic conditions. This provides quantitative decision-making support for selecting buffering materials and implementing site-specific, life-cycle optimized energy-efficiency designs for buildings.

3. Calculation

3.1. Condition

As previously outlined, among the five climate zones, the Hot Summer and Cold Winter Zone exhibits the most substantial material efficiency and carbon reduction benefits. Therefore, this study selects a university teaching building within this climate zone as a case study to conduct an in-depth analysis of the economic benefits and carbon reduction potential of the six materials in practical applications.

The case study focuses on the No.7 Teaching Building at Hunan Agricultural University, located in Hunan Province, China (longitude: 113.08° E, latitude: 28.18° N). This region is characterized by concurrent rainfall and high temperatures, abundant annual mean precipitation, and relatively high humidity, placing it within a typical Hot Summer and Cold Winter Zone. Climatic data indicate that extreme summer temperatures can exceed 40 °C, whereas extreme winter temperatures may fall below 0 °C, as shown in Figures 7 and 8, which were generated using software Ladybug 1.5.0.

The case-study building consists of two distinct structures, separated by a distance of 28.8 m and linked by a connecting corridor. Each structure has a floor area of 4038.66 m^2 and a ceiling height of 3.6 m. The window-to-wall ratio for classrooms and lounges is 21.67%. Functionally, the building includes classrooms, rest areas, toilets, staircases, and an open corridor, as shown in Figure 9.

The initial configurations of the external and internal wall structures of the building are shown in Figure 10. A modeling diagram of the case teaching building is shown in Figure 11.

3.2. Energy Consumption Calculation

In the Hot Summer and Cold Winter Zone, the air conditioning systems of university teaching buildings generally consist of two wall-mounted air conditioning units, and their power specifications are detailed in Table 7. The air conditioning energy consumption in this study was mainly simulated using EnergyPlus 22.2.0.

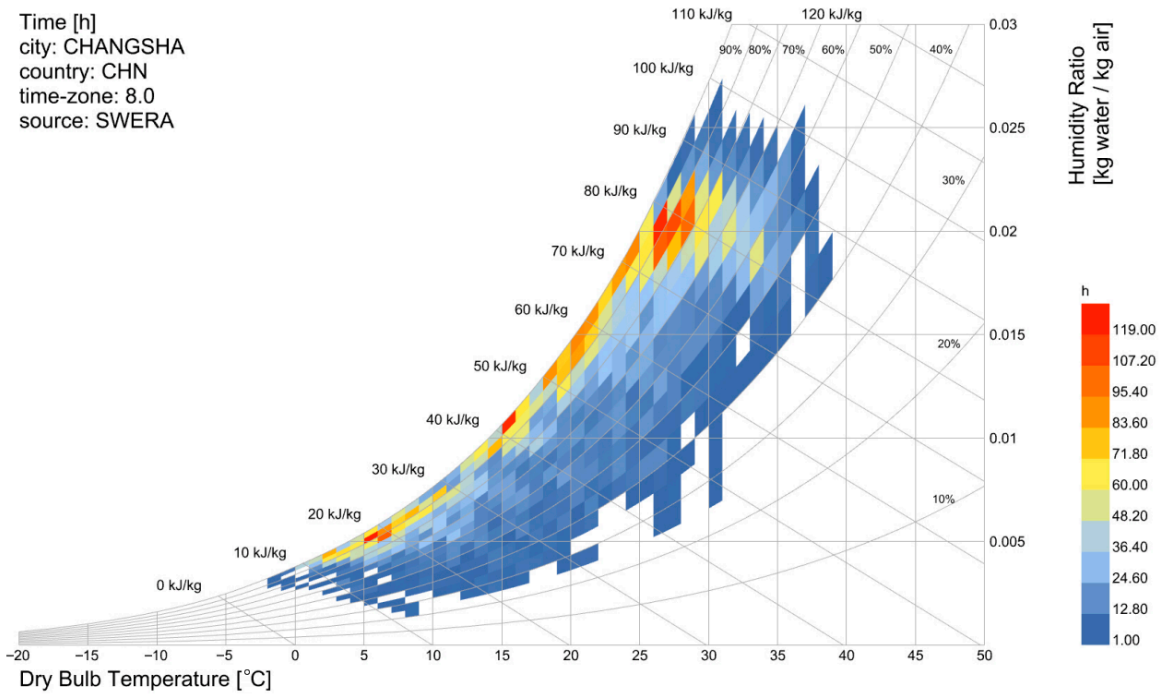


Figure 7. The enthalpy-humidity diagram of Changsha in 2024.

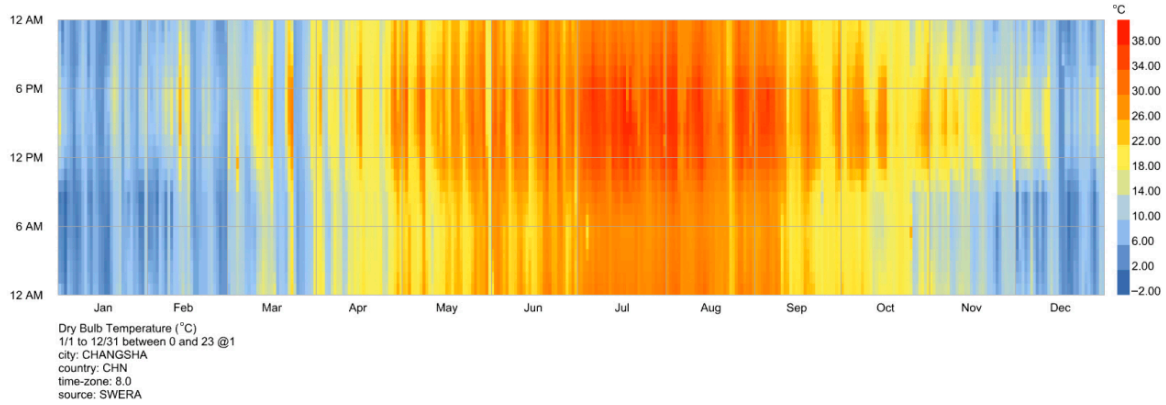


Figure 8. The Dry-Bulb Temperature of Changsha in 2024.

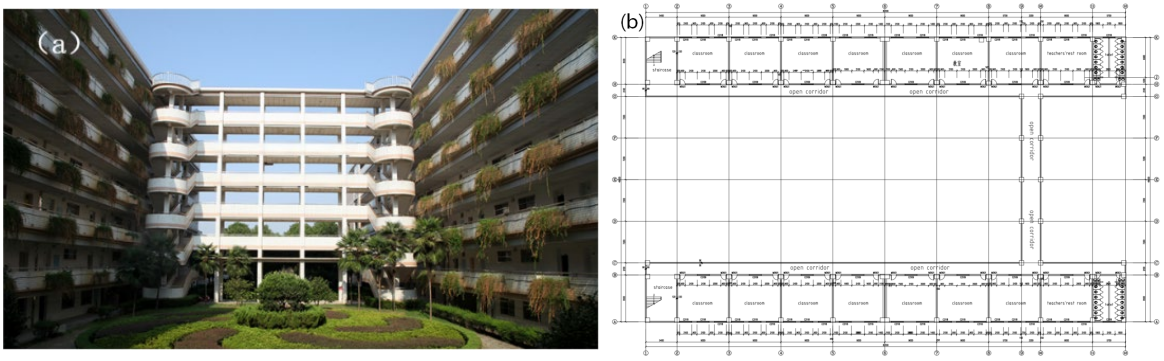


Figure 9. Teaching building diagram: (**a**) building elevation drawings and (**b**) standard floor plans of the building.

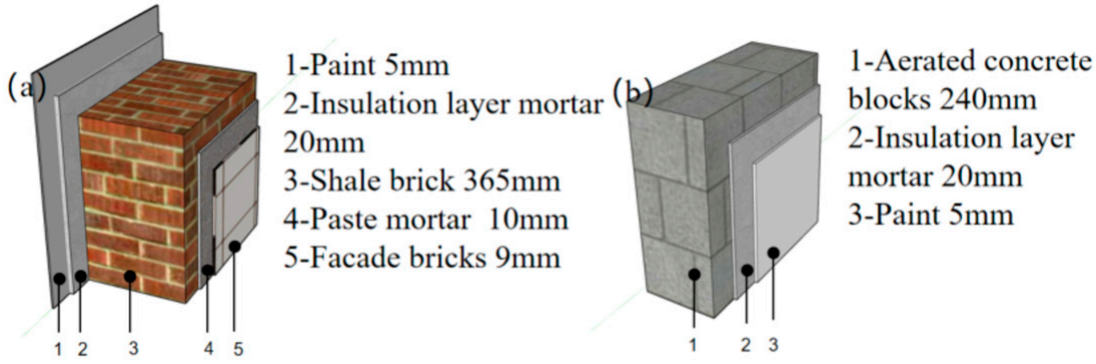


Figure 10. Case building wall structures: (**a**) external wall and (**b**) internal wall.

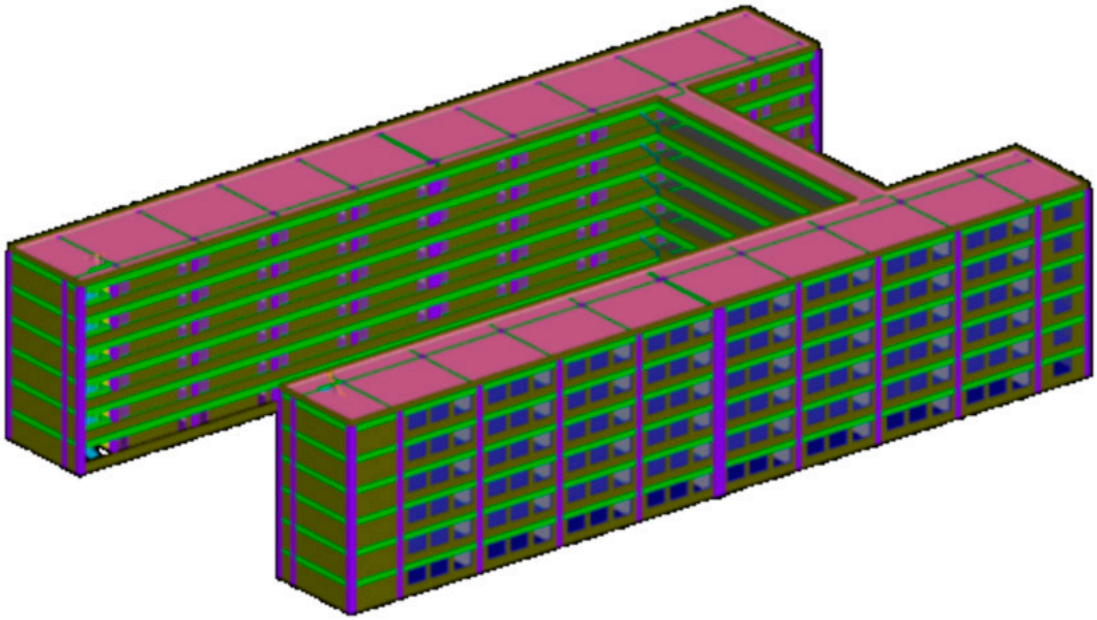


Figure 11. Modeling diagram of the case building.

Table 7. Detailed data of air conditioning in the summer and winter [62].

Cooling Capacity (W)	Summer Cooling Power (W)	Cooling Energy Consumption Ratio	Heating Capacity (W)	Winter Heating Power (W)	Heating Energy Consumption Ratio
3500	1080	3.28	3850	1120	3.44

When utilizing EnergyPlus to simulate building energy consumption, establishing a rational air conditioning system operation strategy is crucial. Although "Design standard for energy efficiency of public buildings" (GB50189-2015 [55]) provides guidelines for parameters such as indoor temperatures in air conditioned zones and classroom vacancy rate, due to the characteristics of university teaching buildings—such as highly variable and irregular occupancy patterns, extended operating hours, and frequent usage during weekends and holidays—strictly following this standard to set air conditioning operation strategies may result in inaccuracies in energy consumption predictions. Therefore, this study examined the air conditioning management systems of nearly 20 university teaching buildings in the Hot Summer and Cold Winter Zone by integrating data from official website reviews with field investigations. Based on the "Design standard for energy efficiency of public buildings" (GB50189-2015 [55]), an air conditioning system operation strategy better aligned with the actual usage patterns of Hot Summer and Cold Winter Zone teaching buildings was formulated. It primarily consists of the following three components.

3.2.1. Determine the Air Conditioning Operating Period

Research indicates that universities typically initiate air conditioning for heating when the daily average outdoor temperature drops below 8 °C, and for cooling when it rises above 26 °C. Based on these findings, this study proposes the following strategy for determining air conditioning operating periods: The heating mode is activated when the daily minimum outdoor temperature drops below 8 °C, and the cooling mode is activated when the daily maximum outdoor temperature exceeds 26 °C. To effectively differentiate short-term meteorological fluctuations from stable operational cycles, a dynamic method for determining the start and end times of air conditioning operation is adopted, based on the climatological concept of "pentad temperature". Specifically, the onset of a heating or cooling period is defined by five consecutive days that meet the corresponding temperature threshold, while the end of the cycle is determined by five consecutive days that falling below the same threshold. Taking Changsha as a case study, Table 8 presents the distribution of its cooling and heating periods over the past decade.

Table 8. Cooling and heating period in Changsha in the past decade.

	Heating Start Time	Heating End Time	Cooling Start Time	Cooling End Time
2014	14 November	15 March	1 May	27 October
2015	30 November	12 March	26 April	27 October
2016	23 November	14 March	28 April	6 October
2017	22 November	16 March	14 April	10 October
2018	18 November	22 March	18 April	7 October
2019	18 November	25 March	6 April	1 November
2020	18 November	1 April	15 April	15 September
2021	22 November	23 March	29 April	5 November
2022	21 November	15 March	6 April	25 October
2023	29 November	20 March	12 April	5 November

The start and end dates of the cooling and heating periods were sorted. After excluding the maximum and minimum values, the median of the remaining dates was computed. Moreover, the winter vacation period (15 January to 15 February) and the summer vacation period (1 July to 1 September) were excluded to determine the annual cooling and heating periods, as presented in Table 9.

Table 9. Changsha cooling and heating time of the year.

Heating Period I	Winter Vacation	Heating Period II	Heating Period III	Heating Time
1 January~15 January	15 January~15 February	15 February~18 March	21 November~31 December	85 days
Cooling period I	Summer vacation	Cooling period II		Cooling time
15 April~1 July	1 July~1 September	1 September~26 October		126 days

3.2.2. Determine Temperature Control Strategy

Based on the actual operational characteristics of university teaching buildings and in accordance with the "Design standard for energy efficiency of public buildings" (GB50189-2015 [55]), a temperature control strategy was developed, as presented in Table 10.

Table 10. Teaching building indoor temperature in air-conditioned area (°C) [55].

Operating Period	Operating Mode	Indoor Set Temperature of Heating and Air Conditioning Zone (°C) at the Following Calculation Moments (h)											
		1	**2**	**3**	**4**	**5**	**6**	**7**	**8**	**9**	**10**	**11**	**12**
Workdays	Cooling	37	37	37	37	37	37	28	26	26	26	26	26
	Heating	5	5	5	5	5	12	18	20	20	20	20	20
Holidays	Cooling	37	37	37	37	37	37	37	37	37	37	37	37
	Heating	5	5	5	5	5	5	5	5	5	5	5	5
Operating period		13	14	15	16	17	18	19	20	21	22	23	24
Workdays	Cooling	26	26	26	26	26	26	26	37	37	37	37	37
	Heating	20	20	20	20	20	20	20	18	5	5	5	5
Holidays	Cooling	37	37	37	37	37	37	37	37	37	37	37	37
	Heating	5	5	5	5	5	5	5	5	5	5	5	5

3.2.3. Determine Classroom Vacancy Rate

In accordance with the "Design Standard for Energy Efficiency of Public Buildings" (GB50189-2015 [55]), and considering the actual operational characteristics of university teaching buildings, the vacancy rates are presented in Table 11. Since certain university classrooms are still used for teaching on weekends, the vacancy rate on weekends is 50% higher than that on weekdays. Given that the course load during the 20:00–21:00 time slot accounts for only 20% to 30% of the average daytime load, the vacancy rate is set at 70%. During non-instructional hours (0:00–7:00, 12:00–14:00, and 18:00–19:00), the vacancy rate is 100%.

Table 11. Teaching building vacancy rates(%).

	Classroom Vacancy Rate for the Following Calculation Moments (h)											
Operating period	1	2	3	4	5	6	7	8	9	10	11	12
Workdays	100	100	100	100	100	100	90	50	50	50	50	100
Holidays	100	100	100	100	100	100	95	75	52.5	52.5	52.5	100
Operating period	13	14	15	16	17	18	19	20	21	22	23	24
Workdays	100	50	50	50	70	70	70	70	100	100	100	100
Holidays	100	52.5	52.5	52.5	85	85	85	85	100	100	100	100

3.3. Indicator Calculation for the Teaching Building

Taking the case building as a reference, the life-cycle costs and life-cycle carbon emissions of the six materials were calculated, accounting for material recycling during the demolition and disposal stage, and the results are presented in Table 12. The baseline group represents the electricity consumption and corresponding carbon dioxide emissions during the building's operation and maintenance stage in the absence of insulation materials. Compared to the single-story residence buildings examined in Section 2.3, the operation and maintenance stage of the teaching building contributes a significantly higher share of both life-cycle costs and life-cycle carbon emissions, accounting for over 95%. Consequently, in the life-cycle assessment of buffering materials, particularly for large public buildings characterized by high energy consumption intensity, it is crucial to prioritize their influence on the building's operational energy demand.

In terms of energy savings, both board-type and cement-based buffering materials reduced more building operational energy consumption compared to the control group (CM). Notably, WPM and BWPM achieved an energy reduction rate of over 18%, which can be attributed to their combined humidity regulation and thermal insulation capabilities.

Table 12. Carbon emissions and costs of the six materials at each stage of the teaching building (when recycling).

Group	Material	Life-Cycle Stage	Cost (10,000 CNY)	Carbon Emission (tCO_2e)
Baseline	-	Operation and Maintenance	2567.294	19,810.618
		Materialization	35.977	65.002
Control	CM	Operation and Maintenance	2562.372	19,772.640
		Demolition and Disposal	−0.509	0.085
		Materialization	68.138	135.230
Board-type	XPS	Operation and Maintenance	2448.381	18,893.020
		Demolition and Disposal	−1.479	−7.189
		Materialization	79.922	131.927
	EPS	Operation and Maintenance	2465.792	19,027.372
		Demolition and Disposal	−2.423	−14.611
		Materialization	80.251	165.982
Cement-based	EM	Operation and Maintenance	2514.673	19,404.566
		Demolition and Disposal	−0.638	0.107
		Materialization	69.144	210.363
	WPM	Operation and Maintenance	2094.609	16,163.126
		Demolition and Disposal	−0.200	0.033
		Materialization	51.261	131.871
	BWPM	Operation and Maintenance	2088.223	16,113.850
		Demolition and Disposal	−0.192	0.032

However, certain materials can reduce energy consumption during building operations and maintenance does not necessarily indicate their economic feasibility or carbon emission reduction benefits. For instance, cement-based buffering material EM exhibits excellent thermal insulation properties, with a thermal conductivity coefficient of 0.0974 W/(m·K)). Compared to the baseline group, the use of EM reduces operational and maintenance costs by 526,210 CNY and lowers carbon emissions during the operational stage by 406.052 tCO_2e. However, due to the relatively high production cost (1042 CNY/m^3) and the necessity of applying an additional base mortar coating prior to construction, which further increases construction expenses, its life-cycle cost reaches 21.63553 million CNY, surpassing the baseline group's 25.67294 million CNY. Consequently, the adoption of EM actually increases the cost of a building's life-cycle. Even with their favorable thermal performance, they still do not offer advantages in life-cycle cost analysis. Despite its economic performance and carbon-reduction potential across different climate zones, lower thermal conductivity in wall materials does not necessarily imply superior economic efficiency or lower carbon emissions. Instead, a comprehensive assessment based on factors such as cost and carbon emission factors is required.

It should be noted that, due to the high vacancy rate in the teaching building for much of the time, the full energy-saving potential of buffering materials may not be effectively realized under these conditions, particularly for the two moisture-buffering plastering mortars (WPM and BWPM). Consequently, the energy-saving performance of these buffering mortars in the teaching building is less significant than that in the detached single-story building described in Section 2.3. Therefore, buffering materials are more suitable for building types characterized by continuous occupancy and higher demands on indoor thermal comfort, such as residential buildings and hotels.

The economic performance indicators for the six materials are summarized in Table 13, while the corresponding carbon reduction indicators are provided in Table 14. The results indicate that opting for material recycling instead of direct landfilling at the end of the building's service life can significantly reduce the material's life-cycle costs and improve the

economic viability of the materials. Specifically, during the demolition and disposal stage, material recycling leads to reductions in both total life-cycle costs and carbon emissions, compared to direct landfill, thereby improving the materials' economic feasibility and carbon reduction potential.

Table 13. Economic dimension indicators of materials in teaching buildings (C_{loss} and $C_{payback}$).

Disposal Method	Indicator	Control	Board-Type		Cement-Based		
		CM	XPS	EPS	EM	WPM	BWPM
Landfilling	C_{loss} (10,000 CNY)	−33.9	47.6	18.3	−31.1	402.4	426.8
	$C_{payback}$ (Year)	394.0	30.0	41.0	79.6	7.4	5.5
Recycling	C_{loss} (10,000 CNY)	−30.5	52.3	24.0	−27.0	403.7	428.0
	$C_{payback}$ (Year)	360.3	28.0	38.2	75.6	7.3	5.3

Table 14. Carbon reduction dimension indicators of materials in teaching buildings (CE_{loss} and $CE_{payback}$).

Disposal Method	Indicator	Control	Board-Type		Cement-Based		
		CM	XPS	EPS	EM	WPM	BWPM
Landfilling	CE_{loss} (tCO_2e)	−36.3	771.8	640.3	228.5	3433.5	3561.4
	$CE_{payback}$ (Year)	97.8	7.9	9.1	21.9	2.9	1.8
Recycling	CE_{loss} (tCO_2e)	−27.1	789.6	665.9	240.0	3437.1	3564.9
	$CE_{payback}$ (Year)	85.7	7.0	7.5	20.5	2.9	1.8

In terms of economic viability, for the control group (CM), both landfilling and recycling scenarios yield negative C_{loss} values below 0, with $C_{payback}$ consistently exceeding the building's design service life (50 years). This indicates that CM is not economically feasible.

For the two board-type buffering materials (XPS and EPS), despite their relatively high initial construction costs, their excellent thermal insulation performance enables reductions in operational energy consumption. This ultimately translates to positive economic benefits, with ($C_{loss} > 0$).

For the cement-based buffering materials (WPM and BWPM), both landfilling and recycling disposal scenarios result in positive C_{loss} values and $C_{payback}$ periods below the building's design service life, indicating favorable economic feasibility over the entire life-cycle. Under the recycling scenario, the WPM and BWPM values amount to 4.024 million CNY and 4.268 million CNY, respectively, exceeding those of the other three buffering materials, which highlights their advantage in reducing the building life-cycle cost. In contrast, despite its excellent thermal performance that reduces operational energy consumption, EM exhibits a negative C_{loss} due to its excessively high construction cost.

The analysis of this case reveals that among the six materials, the economic hierarchy is: BWPM > WPM > XPS > EPS > EM > CM.

In terms of carbon reduction potential, for the control group (CM), both landfilling and recycling scenarios result in CE_{loss} values below zero, with $CE_{payback}$ periods consistently exceeding the building's design service life (50 years). This demonstrates that CM lacks carbon reduction potential.

For the two board-type buffering materials (XPS and EPS), their excellent thermal performance effectively reduces the building's operational energy consumption, resulting in life-cycle carbon emission reductions of up to 789.6 tCO_2e (XPS) and 665.9 tCO_2e (EPS).

For the cement-based buffering materials (EM, WPM, and BWPM), both landfilling and recycling disposal scenarios yield positive CE_{loss} values and $CE_{payback}$ below the building's design service life, indicating a strong potential for carbon reduction over their full life cycle. Under the recycling scenario, the three materials—EM, WPM, and BWPM—achieve total building life-cycle carbon emission reductions of 240.0 tCO_2e, 3437.1 tCO_2e and 3564.9 tCO_2e, respectively.

The analysis of this case reveals that among the six materials, the carbon reduction hierarchy is: BWPM > WPM > XPS > EPS > EM > CM.

In summary, the case study on building construction demonstrates that all five selected buffering materials have carbon-reduction potential and can effectively reduce carbon emissions throughout the entire life cycle of the building. Except for EM, the other four buffering materials are economically feasible and can reduce the building's total life-cycle cost. Among these, the two moisture-buffering plastering mortars (WPM and BWPM) show a particularly strong performance: they reduce life-cycle costs by 15.7% and 16.7%, respectively, while reducing life-cycle carbon dioxide emissions by 17.3% and 18.0%, respectively. These materials therefore bring about dual environmental and economic benefits.

4. Conclusions

This study builds on Life-Cycle Assessment (LCA) and Life-Cycle Cost (LCC) method, integrating key factors: thermal performance, cost, and carbon emissions for wall materials. An enhanced evaluation framework using four novel composite indicators was established. This enabled a systematic assessment of the economic viability and carbon-reduction potential of buffering materials. Five wall materials were analyzed: board-type buffering materials (extruded polystyrene (XPS) boards and Expanded polystyrene (EPS) boards) and cement-based buffering materials (Expanded perlite insulation mortar (EM), Wood-Plastic buffering plastering mortar (WPM), and Bamboo-Wood-Plastic buffering plastering mortar (BWPM)), across five climatic zones in China. A university teaching building in the Hot Summer and Cold Winter Zone was chosen as a case study to assess the real-world performance of these materials. The main conclusions are as follows:

The calculations for different climate zones demonstrate that:

(1) Within the same climatic zone, different buffering materials exhibit variations in carbon emissions and life-cycle costs across the materialization, operation and maintenance, and demolition and disposal stages. A consistent finding is that the operation and maintenance stage accounts for over 90% of total carbon emissions and life-cycle costs across all materials. Therefore, life-cycle assessments of buffering materials should prioritize the impacts of this stage.

(2) Of the two board-type buffering materials, XPS and EPS exhibit consistent advantages in both carbon emission reduction and cost-effectiveness across all climatic zones. Among the three cement-based buffering materials, EM shows carbon reduction potential but lacks economic competitiveness in certain climate zones. For WPM and BWPM, both their economic viability and carbon reduction potential are highly dependent on climatic conditions. In hot–humid zones (Hot Summer and Cold Winter Zone, Hot Summer and Warm Winter Zone), their economic benefits and carbon reduction potential are superior to those of board-type buffering materials and CM. Conversely, in cold and temperate zones (Severe Cold Zone, Cold Zone, and Temperate Zone), the comprehensive performance of board-type buffering materials outperforms that of cement-based buffering materials.

(3) Superior thermal insulation does not inherently imply economic viability. Taking EM as an example, although it exhibits a low thermal conductivity (0.0974 W/(m·K)) and excellent insulating properties, which contribute to reduced energy consumption during the building operation and maintenance stage, its high production cost (1042 CNY/m^3) and the necessity of pre-coating with base mortar during installation lead to increased construction expenses. Therefore, even with its favorable thermal performance, EM does not demonstrate an advantage in full life-cycle cost assessment.

The calculations for the case-study building demonstrate that:

(4) Compared to the control group (CM), all buffering materials effectively reduce the operational energy consumption of buildings. Notably, the two moisture buffering plastering mortars (WPM and BWPM) achieve an operational energy reduction rate exceeding 18%, which can be attributed to their superior synergistic performance in humidity regulation and thermal insulation.

(5) Among the two board-type buffering materials, XPS and EPS demonstrate net life-cycle cost savings and carbon emission reductions. Although these two materials entail relatively high initial costs, their excellent thermal insulation performance offsets this disadvantage. Under the recycling scenario, XPS and EPS achieve life-cycle cost savings of 52.3 million CNY and 24.0 million CNY, respectively, alongside carbon emission reductions of 789.6 tCO_2e and 665.9 tCO_2e.

(6) Among the three cement-based buffering materials, EM can reduce the building's operational energy consumption; however, its high construction costs ultimately result in an increased net life-cycle cost (C_{loss}: −0.27 million CNY). For both WPM and BWPM, both landfilling and recycling scenarios exhibit strong economic viability over the life cycle and significant potential for carbon emission reduction (and greater than 0; and less than the building's design service life). When recycling is implemented during the demolition and disposal stage, EM, WPM, and BWPM achieve life-cycle cost changes of −0.27 million CNY, 4.024 million CNY, and 4.268 million CNY, respectively, alongside carbon emission reductions of 240.0 tCO_2e, 3437.1 tCO_2e, and 3564.9 tCO_2e.

The enhanced evaluation framework proposed in this study addresses the limitations of conventional LCC/LCA methods in assessing the comprehensive life-cycle benefits of buffering materials, while offering practical theoretical tools and decision-making support for the evidence-based selection of buffering materials and for optimizing low-carbon building design. Therefore, future research should expand along two key directions. First, expand coverage to include more detailed climatic zoning and a wider range of building types. Second, integrate long-term durability and dynamic performance degradation into the evaluation system to enhance its decision-support capabilities throughout the entire life-cycle of buildings.

Author Contributions: X.Z.: funding acquisition, validation, writing—original draft, resources; X.W.: software, investigation; writing—review and editing; L.W.: conceptualization, funding acquisition, methodology; Y.C.: data curation; X.F.: supervision; Y.W.: conceptualization; investigation. All authors have read and agreed to the published version of the manuscript.

Funding: This work was supported by Hunan Provincial Department of Water Resources—Research on Formula Optimization and Performance Evaluation System of Ecological Concrete for River Water Quality Purification Based on the Dual Carbon Goal [grant number XSKJ2024064-44]; Hunan Provincial department of education—Study on comprehensive performance of expanded perlite based bamboo fiber buffering plastering mortar [grant number 24C0072] and Hunan Agriculture University—Postgraduate Research Innovation Project [grant number 2024XKCB035].

Data Availability Statement: The datasets used and/or analyzed during the current study are available from the corresponding author upon reasonable request.

Conflicts of Interest: We declare that we have no financial and personal relationships with other people or organizations that can inappropriately influence our work. There is no professional or other personal interest of any nature or kind in any product, service and/or company that could be construed as influencing the position presented in the manuscript entitled.

References

1. World Meteorological Organization. *WMO Confirms 2024 as Warmest Year on Record at About 1.55 °C Above Pre-Industrial Level*; World Meteorological Organization: Geneva, Switzerland, 2025.
2. da Graça Carvalho, M.; Bonifacio, M.; Dechamps, P. Building a low carbon society. *Energy* **2011**, *36*, 1842–1847. [CrossRef]
3. Mao, X.; Wang, L.; Li, J.; Quan, X.; Wu, T. Comparison of regression models for estimation of carbon emissions during building's lifecycle using designing factors: A case study of residential buildings in Tianjin, China. *Energy Build.* **2019**, *204*, 109519. [CrossRef]
4. China Association of Building Energy Efficiency. Research Report on Building Energy Consumption and Carbon Emissions in China. In *Release of Assessment Results on the Situation of Provincial-Level Building Carbon Peaking*; Professional Committee on Building Energy Consumption and Carbon Emission Data, Ed.; China Association of Building Energy Efficiency: Beijing, China, 2021.
5. Fang, J.Z.; Zhang, H.B.; Ren, P.; He, B.J.; Tang, M.F.; Feng, C. Influence of climates and materials on the moisture buffering in office buildings: A comprehensive numerical study in China. *Environ. Sci. Pollut. Res.* **2022**, *29*, 14158–14175. [CrossRef]
6. Tu, K.K.; Zhang, Z.D.; Dreimol, C.H.; Günther, R.; Zboray, R.; Keplinger, T.; Burgert, I.; Ding, Y. Autonomous humidity regulation by MOF/wood composites. *Mater. Horiz.* **2024**, *11*, 5786–5797. [CrossRef]
7. Li, Z.; Chen, W.; Deng, S.; Lin, Z. The characteristics of space cooling load and indoor humidity control for residences in the subtropics. *Build. Environ.* **2006**, *41*, 1137–1147. [CrossRef]
8. Mendes, N.; Winkelmann, F.C.; Lamberts, R.; Philippi, P.C. Moisture effects on conduction loads. *Energy Build.* **2003**, *35*, 631–644. [CrossRef]
9. Annila, P.J.; Lahdensivu, J.; Suonketo, J.; Pentti, M.; Vinha, J. Need to repair moisture- and mould damage in different structures in finnish public buildings. *J. Build. Eng.* **2018**, *16*, 72–78. [CrossRef]
10. Morakinyo, O.M.; Mokgobu, M.I. Indoor Household Exposures and Associated Morbidity and Mortality Outcomes in Children and Adults in South Africa. *Int. J. Environ. Res. Public Health* **2022**, *19*, 9471. [CrossRef]
11. Datta, A.; Suresh, R.; Gupta, A.; Singh, D.; Kulshrestha, P. Indoor air quality of non-residential urban buildings in Delhi, India. *Int. J. Sustain. Built Environ.* **2017**, *6*, 412–420. [CrossRef]
12. Paynter, S. Humidity and respiratory virus transmission in tropical and temperate settings. *Epidemiol. Infect.* **2015**, *143*, 1110–1118. [CrossRef]
13. Wolkoff, P.; Azuma, K.; Carrer, P. Health, work performance, and risk of infection in office-like environments: The role of indoor temperature, air humidity, and ventilation. *Int. J. Hyg. Environ. Health* **2021**, *233*, 113709. [CrossRef]
14. Zhang, T.S.; Yuan, J.M.; Pang, H.X.; Huang, Z.M.; Guo, Y.Q.; Wei, J.X.; Yu, Q.J. UHPC-XPS insulation composite board reinforced by glass fiber mesh: Effect of structural design on the heat transfer, mechanical properties and impact resistance. *J. Build. Eng.* **2023**, *75*, 106935. [CrossRef]
15. Li, Q.L.; Wei, H.B.; Han, L.L.; Wang, F.Y.; Zhang, Y.P.; Han, S.Y. Feasibility of Using Modified Silty Clay and Extruded Polystyrene (XPS) Board as the Subgrade Thermal Insulation Layer in a Seasonally Frozen Region, Northeast China. *Sustainability* **2019**, *11*, 804. [CrossRef]
16. Li, J.H.; Cao, W.L. The Heat Transfer Coefficient of Recycled Concrete Bricks Combination with EPS Insulation Board Wall. *Math. Probl. Eng.* **2015**, *2015*, 695962. [CrossRef]
17. Niu, F.J.; Jiang, H.Q.; Su, W.J.; Jiang, W.T.; He, J.L. Performance degradation of polymer material under freeze-thaw cycles: A case study of extruded polystyrene board. *Polym. Test.* **2021**, *96*, 107067. [CrossRef]
18. Kowalczyk, L.; Korol, J.; Chmielnicki, B.; Laska, A.; Chuchala, D.; Hejna, A. One More Step towards a Circular Economy for Thermal Insulation Materials-Development of Composites Highly Filled with Waste Polyurethane (PU) Foam for Potential Use in the Building Industry. *Materials* **2023**, *16*, 782. [CrossRef] [PubMed]
19. Hemmati, N.; Mirzaei, R.; Soltani, P.; Berardi, U.; Sheikhmozafari, M.J.; Edalat, H.; Rezaieyan, E.; Taban, E. Acoustic and thermal performance of wood strands-rock wool-cement composite boards as eco-friendly construction materials. *Constr. Build. Mater.* **2024**, *445*, 137935. [CrossRef]
20. Qi, X.J.; Tan, Y.X.; Tan, J.S.; Li, X.H. Methods for improving the thermal performance of thermal bridges of lightweight steel-framed buildings. *PLoS ONE* **2024**, *19*, e0314634. [CrossRef]
21. Yin, C.P.; Zheng, Q.; Zeng, J.C.; Yang, J.S.; Xiao, J.Y. Composite sandwich panel with multifunction of load bearing, heat insulation, and thermal protection. *J. Compos. Mater.* **2015**, *49*, 3077–3087. [CrossRef]
22. Ren, Q.M.; Li, X.Z.; Ji, Y.K.; Ding, X.L.; Sun, Q.; Zhao, P.; Li, F.Q.; Vandeginste, V. Thermal insulation of phenolic resin modified fly ash geopolymer. *Constr. Build. Mater.* **2023**, *409*, 133840. [CrossRef]

23. Saca, N.; Radu, L.; Stoleriu, S.; Dobre, D.; Calotă, R.; Truşcă, R. Investigation of Physical-Mechanical Properties and Microstructure of Mortars with Perlite and Thermal-Treated Materials. *Materials* **2024**, *17*, 3412. [CrossRef]
24. Qi, X.Q.; Bao, Y.F.; Wang, W.R.; Zhang, S.L.; Wu, Y.L.; Jia, Z.Q.; Guo, S.Y. Superior performance foamed concrete fabricated with amphiphilic and hydrophilic particles stabilized ultra-stable foam. *Cem. Concr. Compos.* **2024**, *152*, 105613. [CrossRef]
25. Gong, J.Q.; Duan, Z.R.; Sun, K.Q.; Xiao, M. Waterproof properties of thermal insulation mortar containing vitrified microsphere. *Constr. Build. Mater.* **2016**, *123*, 274–280. [CrossRef]
26. Chen, M.X.; Wang, S.D.; Lu, L.C.; Zhao, P.Q.; Gong, C.C. Effect of matrix components with low thermal conductivity and density on performances of cement-EPS/VM insulation mortar. *J. Therm. Anal. Calorim.* **2016**, *126*, 1123–1132. [CrossRef]
27. Yuan, P.; Zhu, Y.S.; Li, D.H.; Lu, X.F. Effect of Freeze-Thaw Cycle and Moisture Content on Compressive and Energy Properties of Alkali Slag Ceramsite Concrete. *Ksce J. Civ. Eng.* **2024**, *28*, 1980–1991. [CrossRef]
28. Balbuena, J.; Sánchez, M.; Sánchez, L.; Cruz-Yusta, M. Lightweight Mortar Incorporating Expanded Perlite, Vermiculite, and Aerogel: A Study on the Thermal Behavior. *Materials* **2024**, *17*, 711. [CrossRef] [PubMed]
29. Pavlík, Z.; Pokorný, J.; Pavlíková, M.; Zemanová, L.; Záleská, M.; Vyšvařil, M.; Žižlavský, T. Mortars with Crushed Lava Granulate for Repair of Damp Historical Buildings. *Materials* **2019**, *12*, 3557. [CrossRef] [PubMed]
30. Tariku, F.; Kumaran, K.; Fazio, P. Application of a Whole-Building Hygrothermal model in energy, durability, and indoor humidity retrofit design. *J. Build. Phys.* **2014**, *39*, 3–34. [CrossRef]
31. De Rossi, A.; Carvalheiras, J.; Novais, R.M.; Ribeiro, M.J.; Labrincha, J.A.; Hotza, D.; Moreira, R. Waste-based geopolymeric mortars with very high moisture buffering capacity. *Constr. Build. Mater.* **2018**, *191*, 39–46. [CrossRef]
32. Wu, Y.; Gong, G.C.; Yu, C.W.; Huang, Z.Y. Proposing ultimate moisture buffering value (UMBV) for characterization of composite porous mortars. *Constr. Build. Mater.* **2015**, *82*, 81–88. [CrossRef]
33. Dong, Y.H.; Ng, S.T. A modeling framework to evaluate sustainability of building construction based on LCSA. *Int. J. Life Cycle Assess.* **2016**, *21*, 555–568. [CrossRef]
34. Onat, N.C.; Kucukvar, M.; Tatari, O. Integrating triple bottom line input-output analysis into life cycle sustainability assessment framework: The case for US buildings. *Int. J. Life Cycle Assess.* **2014**, *19*, 1488–1505. [CrossRef]
35. Fauzi, R.T.; Lavoie, P.; Sorelli, L.; Heidari, M.D.; Amor, B. Exploring the Current Challenges and Opportunities of Life Cycle Sustainability Assessment. *Sustainability* **2019**, *11*, 636. [CrossRef]
36. Nava, S.; Chalabi, Z.; Bell, S.; Sendra, P.; Burman, E. Identifying the criteria for community-centred Life Cycle Sustainability Assessment of estate regeneration schemes. *Heliyon* **2024**, *10*, e31115. [CrossRef] [PubMed]
37. Larsen, V.G.; Tollin, N.; Sattrup, P.A.; Birkved, M.; Holmboe, T. What are the challenges in assessing circular economy for the built environment? A literature review on integrating LCA, LCC and S-LCA in life cycle sustainability assessment, LCSA. *J. Build. Eng.* **2022**, *50*, 104203. [CrossRef]
38. Zarauz, I.; Sanz-Hernández, A.; Rivera-Lirio, J.M. Social sustainability in a good bioeconomy paradigm: A systematic review of social life cycle assessment (S-LCA). *J. Clean. Prod.* **2025**, *486*, 144570. [CrossRef]
39. Ayassamy, P.; Pellerin, R. Social Life-Cycle Assessment in the Construction Industry: A Review of Characteristics, Limitations, and Challenges of S-LCA through Case Studies. *Sustainability* **2023**, *15*, 14569. [CrossRef]
40. Prakash, V.; Ghosh, S.; Kanjilal, K. Costs of avoided carbon emission from thermal and renewable sources of power in India and policy implications. *Energy* **2020**, *200*, 117522. [CrossRef]
41. Huang, Y.; Niu, J.L.; Chung, T.M. Energy and carbon emission payback analysis for energy-efficient retrofitting in buildings-Overhang shading option. *Energy Build.* **2012**, *44*, 94–103. [CrossRef]
42. Sun, B.D.; Zhong, C.H.; Yu, D.H.; Han, Q.; Tang, J.C. Life cycle carbon emission assessment and carbon payback period analysis for the regeneration of old residential areas in cold regions: Case study in Qingdao, China. *Sustain. Cities Soc.* **2024**, *115*, 105860. [CrossRef]
43. *GB 50176-1993*; Thermal Design Code for Civil Buildings. Ministry of Housing and Urban-Rural Development: Beijing, China, 2017.
44. *GB/T 51366-2019*; Standard for Building Carbon Emission Calculation. China Architecture & Building Research Institute Co., Ltd. (CABR): Beijing, China, 2019.
45. Mushu, F.; Guangcai, G.; Long, L.; Ping, W. Thermodynamic Model for Estimating Energy, Exergy Consumption and CO_2 Emissions in Envelope Production Phase Based on Economic Indicators. *Sci. Technol. Eng.* **2016**, *16*, 75–81.
46. Chen, C.; Wang, M.Y.; Shen, C.Z.; Huang, Y.Y.; Zhu, M.H.; Wang, H.F.; He, L.P.; Julien, D.B. Sensitivity Analysis of Factors Influencing Rural Housing Energy Consumption in Different Household Patterns in the Zhejiang Province. *Buildings* **2023**, *13*, 463. [CrossRef]
47. Kavgic, M.; Mumovic, D.; Summerfield, A.; Stevanovic, Z.; Ecim-Djuric, O. Uncertainty and modeling energy consumption: Sensitivity analysis for a city-scale domestic energy model. *Energy Build.* **2013**, *60*, 1–11. [CrossRef]
48. Peng, C.H.; Li, Z.R.; Xu, Q.Y.; Li, X.R.; Li, X.F.; Chen, H.Y. Spatial distribution of energy consumption: Integrating climate and macro-statistics for insights from clustering and sensitivity analysis. *Energy Build.* **2024**, *318*, 114446. [CrossRef]

49. *GB 50204*; Technical Specification for Plasting Mortar. China Architecture & Building Press: Beijing, China, 2011.
50. Cao, B.; Luo, M.H.; Li, M.; Zhu, Y.X. Too cold or too warm? A winter thermal comfort study in different climate zones in China. *Energy Build.* **2016**, *133*, 469–477. [CrossRef]
51. Chen, X.A.; Yang, J.C.; Ren, C.; Jeong, S.; Shi, Y.A. Standardizing thermal contrast among local climate zones at a continental scale: Implications for cool neighborhoods. *Build. Environ.* **2021**, *197*, 107878. [CrossRef]
52. Dong, Y.; Duan, H.Q.; Li, X.S.; Zhang, R.A. Influence of Different Forms on BIPV Gymnasium Carbon-Saving Potential Based on Energy Consumption and Solar Energy in Multi-Climate Zones. *Sustainability* **2024**, *16*, 1656. [CrossRef]
53. Qian, B.; Yu, T.; Zhang, C.; Heiselberg, P.K.; Lei, B.; Yang, L. Suitability of heat wave event definitions for assessing indoor overheating in current and future climate: A case study in China. *Build. Environ.* **2023**, *241*, 110487. [CrossRef]
54. Yang, W.Y.; Zhao, Y.R.; Liso, V.; Brandon, N. Optimal design and operation of a syngas-fuelled SOFC micro-CHP system for residential applications in different climate zones in China. *Energy Build.* **2014**, *80*, 613–622. [CrossRef]
55. *GB 50189-2015*; Design Standard for Energy Efficiency of Public Buildings. China Architecture & Building Press: Beijing, China, 2015.
56. *GB 50189*; Energy Efficiency Design Standards for Residential Buildings. Tongji University Press: Shanghai, China, 2011.
57. Alimohamadi, R.; Jahangir, M.H. Multi-Objective optimization of energy consumption pattern in order to provide thermal comfort and reduce costs in a residential building. *Energy Convers. Manag.* **2024**, *305*, 118214. [CrossRef]
58. El Samanoudy, G.; Mahmoud, N.S.A.; Jung, C.L. Analyzing the effectiveness of building integrated Photovoltaics (BIPV) to reduce the energy consumption in Dubai. *Ain Shams Eng. J.* **2024**, *15*, 102682. [CrossRef]
59. Idrissi, Y.C.; Belarbi, R.; Ferroukhi, M.Y.; Feddaoui, M.; Agliz, D. Development of a numerical approach to assess the effect of coupled heat and moisture transfer on energy consumption of residential buildings in Moroccan context. *J. Build. Phys.* **2022**, *45*, 774–808. [CrossRef]
60. *GB 50736-2012*; Design Code for Heating Ventilation and Air Conditioning of Civil Buildings. China Architecture & Building Press: Beijing, China, 2012.
61. Available online: https://rp5.ru/ (accessed on 6 November 2025).
62. Xie, F.; Wu, Y.; Wang, X.; Zhou, X. Optimization Strategies for the Envelope of Student Dormitories in Hot Summer and Cold Winter Regions: Multi-Criteria Assessment Method. *Sustainability* **2024**, *16*, 6172. [CrossRef]

Disclaimer/Publisher's Note: The statements, opinions and data contained in all publications are solely those of the individual author(s) and contributor(s) and not of MDPI and/or the editor(s). MDPI and/or the editor(s) disclaim responsibility for any injury to people or property resulting from any ideas, methods, instructions or products referred to in the content.